PHYSICAL REVIEW B **91**, 081107(R) (2015)

Multiferroicity in orthorhombic $R\mathrm{MnO_3}$ (R = Dy, Tb, and Gd) under high pressure

Takuya Aoyama,[1] Ayato Iyama,[1] Katsuya Shimizu,[2] and Tsuyoshi Kimura[1]

[1]*Division of Materials Physics, Graduate School of Engineering Science, Osaka University, Toyonaka, Osaka 560-8531, Japan*

[2]*KYOKUGEN, Graduate School of Engineering Science, Osaka University, Toyonaka, Osaka 560-8531, Japan*

(Received 18 December 2014; published 18 February 2015)

The hydrostatic pressure effect on multiferroic properties of rare-earth manganites $R\mathrm{MnO_3}$ (R = Dy, Tb, and Gd) with the *Pbnm* orthorhombic structure was investigated by using a diamond anvil cell. Under high pressure, all of these manganites were found to exhibit ferroelectricity in which spontaneous polarization ($\approx 10^0$ μC/cm^2) develops along the a axis. The application of a magnetic field B along the a axis to the high-pressure ferroelectric phase causes a drastic change in the electric polarization P. Especially in $\mathrm{GdMnO_3}$, the B-induced change in P reached $\Delta P(B) = 1.3$ μC/cm^2. A possible origin of the observed R-dependent pressure effect is discussed.

DOI: 10.1103/PhysRevB.91.081107 PACS number(s): 75.85.+t, 74.62.Fj, 62.50.−p

In the past decade, the study of spin-driven ferroelectrics has been attracting a great deal of interest [1–4]. In spin-driven ferroelectrics, their ferroelectricity is induced by a magnetic order breaking the inversion symmetry, and their electric polarization P can be manipulated by a magnetic field, i.e., direct magnetoelectric effect. Though this effect is attractive from a technological point of view, several crucial problems still remain for the use of practical applications. One of the problems is that the effect can be observed only far below room temperature in most spin-driven ferroelectrics. Only a few systems, such as hexaferrite compounds [5], have been found to exhibit spin-driven ferroelectricity at room temperature. Another problem is that the magnitude of P in spin-driven ferroelectrics is much smaller than that in conventional ferroelectrics such as $\mathrm{BaTiO_3}$ ($P \approx 20$ μC/cm^2) [6]. Until 2013, the highest value of spin-driven P was 0.36 μC/cm^2, which was observed in $\mathrm{GdM_2O_5}$ [7] (another example is 0.29 μC/cm^2 in $\mathrm{CaMn_7O_{12}}$ [8]). Recently, however, considerably large spin-driven ferroelectric polarization ($P \approx 1.0$ μC/cm^2) has been reported for a representative spin-driven ferroelectric, $\mathrm{TbMnO_3}$, under high pressure ($\geqslant$ about 4.5 GPa) [9]. In $\mathrm{TbMnO_3}$, a *bc* cycloidal spiral magnetic structure [upper inset of Fig. 1(d)] leads to ferroelectricity along the c axis at ambient pressure via the relativistic inverse Dzyaloshinskii-Moriya (DM) interaction [10–12]. Density functional simulations [9] suggest that the enhancement of P by applying pressure in $\mathrm{TbMnO_3}$ is due to the stabilization of a collinear up-up-down-down spin ordered state, the so-called E-type antiferromagnetic (E-AFM) state [lower inset of Fig. 1(d)], which allows ferroelectricity along the a axis via the nonrelativistic symmetric exchange interaction [13,14]. Though various studies of the high-pressure effect on spin-driven ferroelectrics have been reported [15–18], most of them have not experimentally demonstrated enhancements of their magnetoelectric (ME) activity. However, the high-pressure study on $\mathrm{TbMnO_3}$ reported in Ref. [9] revealed that the application of high pressure can be an effective perturbation to improve the ME performance of spin-driven ferroelectrics.

To further elucidate the pressure effect on the spin-driven ferroelectricity in $\mathrm{TbMnO_3}$ and to pursue better magnetoelectric couplings in high-pressure conditions, we systematically investigated multiferroic properties in perovskite rare-earth manganites $R\mathrm{MnO_3}$ (R = Dy, Tb, and Gd), under pressures up to about 10 GPa. In perovskite $R\mathrm{MnO_3}$ with a $\mathrm{GdFeO_3}$-type distortion, structural modifications through the change in the ionic radius of the R ion (r_R) strongly affect their magnetic ground state [19] and the resulting multiferroic properties [20]. Therefore, systematic high-pressure studies on $R\mathrm{MnO_3}$ with various r_R ($r_{\mathrm{Dy}} < r_{\mathrm{Tb}} < r_{\mathrm{Gd}}$), meaning the simultaneous tuning of physical and chemical pressures, will provide information for further understanding the gigantic spin-driven ferroelectric polarization observed in $\mathrm{TbMnO_3}$ under high pressure. Moreover, it is known that R moments play an important role in the magnetoelectric properties below the Néel temperature of R moments (T_{N}^R). Thus, the present Rapid Communication will also provide an optimum condition to achieve stronger magnetoelectric coupling by tuning the physical and chemical pressures as well as R moments. In the end, we discovered a giant change of P ($\Delta P \approx 1.3$ μC/cm^2) in $\mathrm{GdMnO_3}$.

Single crystals of $R\mathrm{MnO_3}$ (R = Dy, Tb, and Gd) were grown by the floating zone method. Obtained crystals were cut into plate-shaped specimens with a dimension of 150 × 150 × 25 μm^3 and the widest face perpendicular to the a axis (*Pbnm* setting). A diamond anvil cell made of Cu-Be alloy was used to apply pressure to the specimens. Glycerin was used as a pressure transmitting medium, which has been reported to be hard to crystallize, and freezes as a glass at around 5 GPa at room temperature [21]. Therefore, the uniaxiality of applied pressure can be expected to be relatively small in the present study. Pressure was applied at room temperature and determined at room temperature in each measurement by using the ruby fluorescence method [22]. By introducing the diamond anvil cell into a superconducting magnet, a relative dielectric constant ε' at 10 kHz and an electric polarization P were measured in magnetic fields up to 8 T and under pressure up to about 10 GPa. In this study, both electric (E) and magnetic (B) fields were applied only along the a axis. An *LCR* meter and an electrometer were used for the measurements of ε' and P, respectively. More details of the measurements are described in Ref. [23].

Figure 1(a) displays temperature T profiles of ε' normalized by the data at 60 K on $\mathrm{DyMnO_3}$ at various pressures. $\mathrm{DyMnO_3}$ is known to exhibit spin-driven ferroelectricity along the c axis due to the *bc* cycloidal spiral spin order at ambient pressure [20]. At 0.2 GPa (near ambient pressure), the ε'-T curve showed a steady increase from $T_{\mathrm{N}}^{\mathrm{Mn}}$ ($\approx$39 K) and a small kink structure at T_{C} ($\approx$19 K) where the spin-driven ferroelectricity

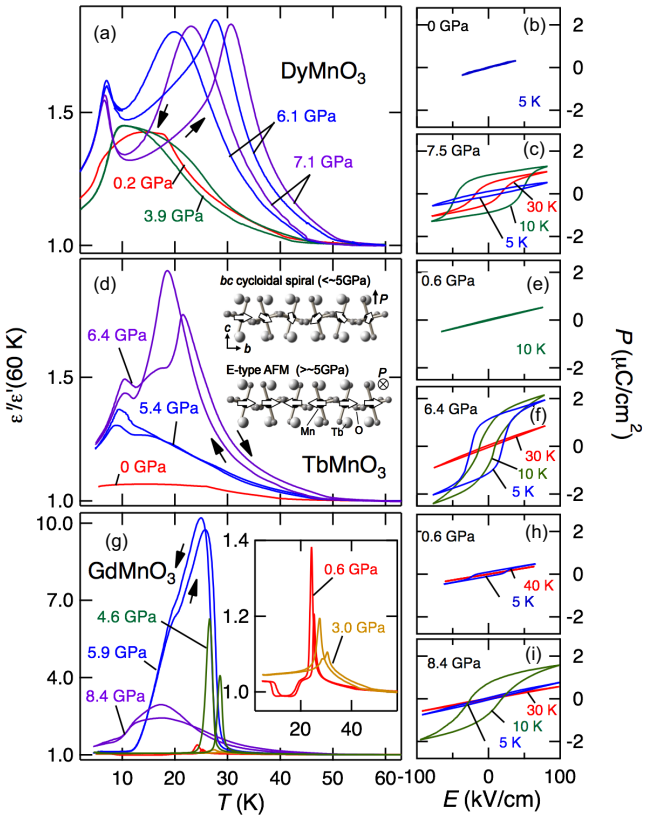

FIG. 1. (Color online) Dielectric and ferroelectric properties of (a)–(c) $DyMnO_3$, (d)–(f) $TbMnO_3$, and (g)–(i) $GdMnO_3$ at various pressures. The left panels show the temperature dependence of the relative dielectric constant ε' normalized by the value at 60 K. The right panels represent electric polarization as a function of applied electric field at selected pressures and temperatures. All the measurements were done with $E\|a$ at 0 T. The data of $TbMnO_3$ are taken from Ref. [9]. The upper and lower insets of (d) show schematic drawings of the *bc* cycloidal spiral and the *E*-type AFM structures, respectively.

emerges. At 3.9 GPa, a thermal hysteretic behavior appears in the ε'-T curve at around 12 K $\leqslant T \leqslant T_N^{Mn}$, and the kink anomaly at T_C vanishes. With further increasing pressure, the ε'-T curve exhibits a more rapid increase below ~45 K (at 6.1 GPa) and ~51 K (at 7.1 GPa), and shows a striking peak feature accompanying a thermal hysteresis and a clear anomaly at $T_N^{Dy} \approx 8$ K. In Fig. 1(b), the P-E curve collected at 5 K and 0 GPa is displayed. At ambient pressure, no hysteresis is observed in P along the a axis since a spontaneous polarization P_s appears along the c axis at ambient pressure. As seen in Fig. 1(c), however, a clear hysteresis loop was observed in the P-E curves at 7.5 GPa. The maximum P_s reached 1 μC/cm^2 at around 7.1 GPa. The magnitude of P_s was steeply suppressed below T_N^{Dy}, as seen in the data at 5 K of Fig. 1(c). The observed pressure effects on the dielectric and ferroelectric properties in $DyMnO_3$ (e.g., enhancement of ε' below T_N^{Mn}, pressure-induced flop of P from c to a, large P_s in the high-pressure phase, and suppression of P_s below T_N^R) are essentially the same as those observed in $TbMnO_3$. [See Figs. 1(d)–1(f). Though the data sets of $TbMnO_3$ have been reported in Ref. [9], they are shown here for a comparison.]

Dielectric and ferroelectric properties in $GdMnO_3$ are slightly different from those in $DyMnO_3$ and $TbMnO_3$. At ambient pressure, the magnetic ground state of $GdMnO_3$ is located at around the boundary of the A-type antiferromagnetic (A-AFM) phase and the spiral magnetic ordered phase with the spiral plane parallel to the ab plane [24,25]. While the A-AFM phase is paraelectric, the ab spiral spin order can induce ferroelectricity with $P\|\|a$ due to the inverse DM mechanism [11]. Thus, the ground state of $GdMnO_3$ has been reported to be either paraelectric [26] or ferroelectric with $P\|\|a$ [27]. Figure 1(g) shows T profiles of normalized ε' under various pressures on $GdMnO_3$. Under low pressures [inset of Fig. 1(g)], a relatively small lambda-shaped anomaly in ε' was observed at 24–28 K which corresponds to a magnetic transition temperature into the A-AFM phase [19]. With increasing pressure, the anomaly is drastically enhanced, and at 5.9 GPa the peak top value of ε' reaches 600. Above 6 GPa, the peak structure is suppressed with increasing pressure [see the 8.4 GPa data of Fig. 1(g)].

Figures 1(h) and 1(i) display the isothermal P-E curves collected at 0.6 and 8.4 GPa, respectively, for $GdMnO_3$. At low pressure (0.6 GPa) and 5 K, small but finite P_s (≈0.09 μC/cm^2) was observed, which is probably ascribed to the development of the ab spiral magnetic order [27]. At 8.4 GPa and 10 K, P_s was remarkably enhanced and its magnitude reached 1 μC/cm^2. The enhancement of P_s appears in accordance with those of ε' shown in Fig. 1(g). It should be noted that the ferroelectricity at the high-pressure phase vanished again below 5 K [Fig. 1(i)], suggesting that the ordering of Gd moments suppresses the ferroelectricity. The ferroelectric characteristics in the high-pressure phase of $GdMnO_3$ [e.g., the large magnitude of P_s (~10^0 μC/cm^2) and the suppression of P_s below T_N^R] are essentially the same with those in $TbMnO_3$ and $DyMnO_3$.

The effects of B on ε'-T and P-E curves in the high-pressure ferroelectric phase were also investigated for all the three manganites. The results are shown in Fig. 2. As shown in the left panels of Fig. 2, a peak structure in the ε'-T curve with thermal hysteresis shifts toward higher T with increasing B in all of the manganites. This suggests that T_C increases with increasing B. It should be also noted that the small peak (or shoulder) around T_N^R (<~10 K) in the ε'-T curves disappears and the magnitude of ε' at the lowest T is considerably suppressed at high B. The inset of Fig. 2(g) shows ε'-T curves of $GdMnO_3$ at 5.9 GPa, where the maximum value of ε' (≈600 at 22 K) was observed. In this pressure, a magnetodielectric effect, i.e., B-induced change in ε',$[\varepsilon'(8\text{ T}) - \varepsilon'(0\text{ T})]/\varepsilon'(0\text{ T}) = -740\%$, was observed at 24 K. Such remarkable enhancements of ε' and the magnetodielectric effect were reported in systems at which the ab- and bc-cycloidal phases compete with each other (e.g., $Tb_{1-x}Gd_xMnO_3$ at 0 T [28] and $DyMnO_3$ at $B\|b$ [20,29]). Since $GdMnO_3$ is located near the phase boundary between the ab- and bc-cycloidal phases [28], the local motion of the multiferroic domain wall as discussed in $DyMnO_3$ at $B\|b$ [29] can be attributable to the dielectric enhancements observed in the 5.9 GPa data.

As displayed in the right panels of Fig. 2, the P-E hysteresis loop (or P_s) in the high-pressure phase becomes larger by

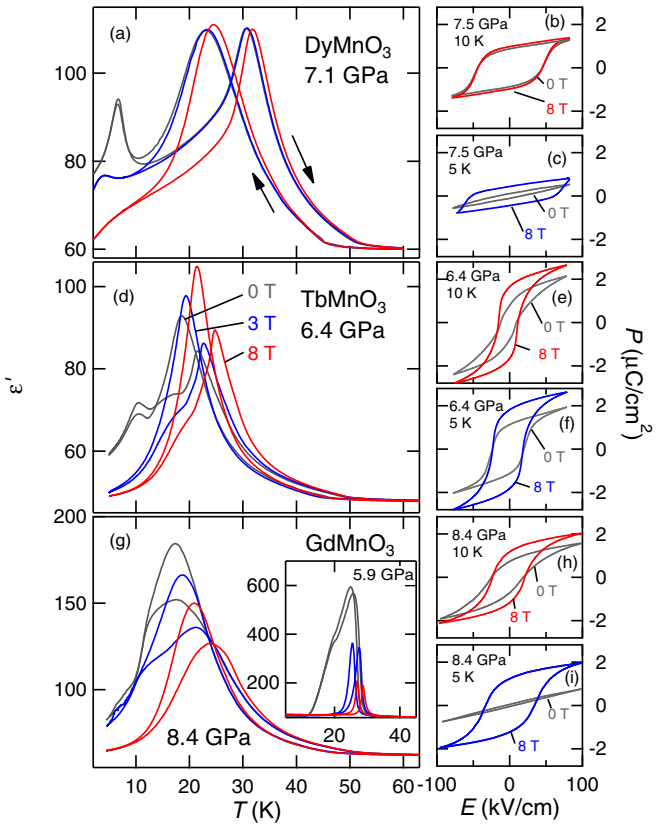

FIG. 2. (Color online) Dielectric and ferroelectric properties in the high-pressure phase of (a)–(c) $DyMnO_3$, (d)–(f) $TbMnO_3$, and (g)–(i) $GdMnO_3$ at several magnetic fields. The left panels show the temperature dependence of relative dielectric constant ε'. The right panels represent electric polarization as a function of applied electric field at selected pressures, temperatures, and magnetic fields. Both E and B were applied along the a axis.

applying B for all the three manganites. The B-induced enhancement of the P-E loop (or P_s) is more pronounced at 5 K ($<T_N^R$) than 10 K ($>T_N^R$), especially for $DyMnO_3$ and $GdMnO_3$, in which P_s is steeply suppressed below T_N^R in the absence of B. Thus, ε' and P clearly showed a remarkable B dependence below T_N^R in the high-pressure phase of all the three manganites studied here.

To further elucidate the B effect on ε' and P in the high-pressure phase, we measured the isothermal magnetodielectric (MD) and magnetoelectric (ME) effects. The left panels of Fig. 3 display the B dependence of ε' collected at 5 K ($<T_N^R$) in the low-pressure (red curves) and high-pressure (blue curves) phases. For all the manganites, a sudden change in ε' was observed at $B_m = 2-4$ T in both the low- and high-pressure phases. For $DyMnO_3$ and $TbMnO_3$, the B-induced change in ε' at B_m is positive in the low-pressure phase ($P \| c$ phase) while that in the high-pressure phase ($P \| a$ phase) is negative. In contrast, that in $GdMnO_3$ is negative in both the low- and high-pressure phases. Note that both the low- and high-pressure phases in $GdMnO_3$ exhibit ferroelectricity along the a axis. Therefore, we can conclude that the sign of the MD effect at B_m is always negative in the manganites studied here when P is parallel to the a axis.

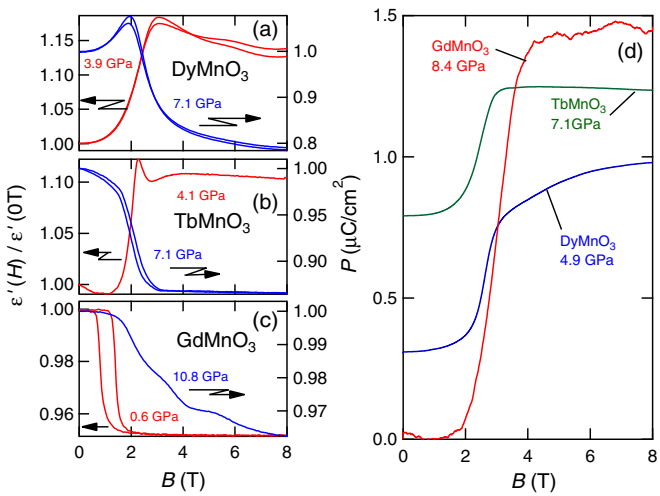

FIG. 3. (Color online) Magnetodielectric effect at 5 K($<T_N^R$) in the low-pressure (red curves) and high-pressure (blue curves) phases of (a) $DyMnO_3$, (b) $TbMnO_3$, and (c) $GdMnO_3$. (d) Magnetoelectric effect at 5 K in the high-pressure phase of these manganites. Both E and B were applied along the a axis.

Accompanied by this negative MD effect, a nonlinear ME effect was also observed. Figure 3(d) shows P as a function of B at 5 K in the high-pressure phase of the three manganites. These data were taken in B-decreasing runs. In all of them, a strong enhancement of P was observed at $B_m = 2-4$ T. This trend, i.e., B enhancement of P, is consistent with the results obtained from P-E hysteresis curves (see the right panels of Fig. 2). It is worth mentioning that the observed B-induced change in P on $GdMnO_3$ reaches $\Delta P = 1.3\ \mu C/cm^2$, which is more than twice the high value reported in spin-driven ferroelectrics (cf. $\Delta P \approx 0.5\ \mu C/cm^2$ in $GdMn_2O_5$ [7] and the high-pressure phase of $TbMnO_3$ [9]). This result demonstrates that the gigantic spin-driven ferroelectric polarization can be magnetically controlled. Though a remarkable ME effect was observed below T_N^R in the high-pressure phase of all the manganites studied here, its microscopic mechanism is still unclear. To further verify the mechanism, more microscopic information such as crystallographic and magnetic structures at a magnetic field, high pressure, and low temperature will be required.

Let us summarize the experimental results. Figure 4 displays the pressure dependence of the spontaneous polarization along a at several temperatures in $B = 0$ T (left panels) and 8 T (right panels) for the manganites studied here. It is evident that all the manganites show a strong enhancement of P by the application of high pressure. The observed ME characteristics in the high-pressure phase [e.g., the magnitude and the direction of P ($\approx 10^0\ \mu C/cm^2 \| a$), suppression of P below T_N^R in $B = 0\ T$, and recovery of the magnitude of P below T_N^R by applying high B] are essentially common in all three manganites. This suggests that the high-pressure phase of $GdMnO_3$ and $DyMnO_3$ will be the same as that in $TbMnO_3$, in which the pressure-induced transition into the E-AFM phase has been proposed by powder neutron diffraction [30] and density functional simulation studies [9]. It is also worth mentioning that the critical pressure at which a

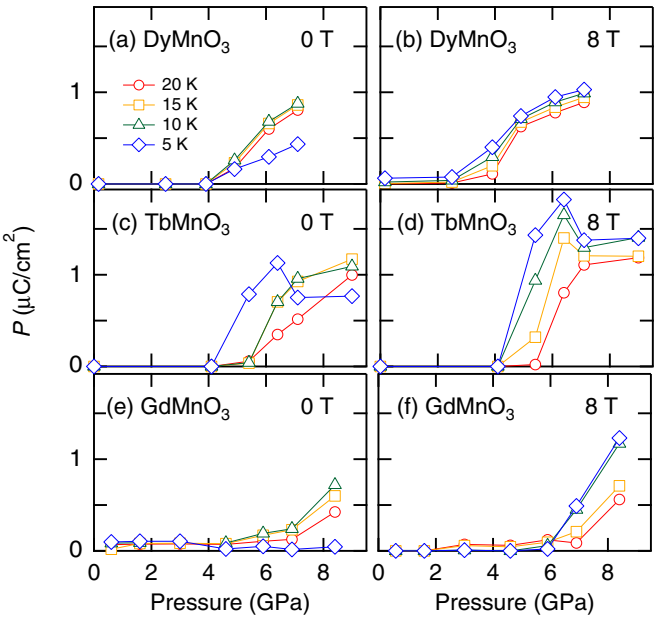

FIG. 4. (Color online) The spontaneous polarization as a function of pressure at several temperatures in magnetic fields of 0 T (left panels) and 8 T (right panels) for $DyMnO_3$ (top), $TbMnO_3$ (middle), and $GdMnO_3$ (bottom).

steep increase of P along a is observed, and probably at which the pressure-induced ME transition into the E-type AFM phase takes place, becomes smaller with decreasing r_R. Such r_R dependence of the critical pressure is consistent with the fact that the ground state of $HoMnO_3$ with smaller r_R is E-AFM at ambient pressure [31], and can be reasonably explained in terms of the stabilization of the E-AFM phase in $RMnO_3$ with smaller r_R at ambient pressure [32].

To conclude, the effect of pressure up to about 10 GPa and magnetic fields up to 8 T on multiferroicity in orthorhombic $RMnO_3$ (R = Dy, Tb, and Gd) has been investigated by using a diamond anvil cell installed at a superconducting magnet. All of these manganites are found to show a pressure-induced phase transition into the phase with large spin-driven ferroelectric polarization along the a axis. The ferroelectricity can be reasonably interpreted in terms of the development of the E-type antiferromagnetic order by applying pressure. By comparing the critical pressure for the pressure-induced transition of these manganites, we found that the critical pressure increases with increasing the ionic radius of R. In addition, the high-pressure phase of these manganites exhibits a large direct magnetoelectric effect accompanied by a metamagnetic transition related to R moments. At the transition caused by the application of a magnetic field, the magnitude of the ferroelectric polarization drastically changes. In particular, $GdMnO_3$ shows a huge magnetic-field-induced change in the polarization ($\Delta P = 1.3\ \mu C/cm^2$). Though the presently observed large spin-driven ferroelectric polarization and magnetoelectric effect are achieved only at high pressure, the result will provide some clues to enhance magnetoelectric couplings and multiferroic functionalities in spin-driven ferroelectrics.

We thank A. Miyake, K. Kimura, and Y. Wakabayashi for enlightening discussions. This work was supported by Grant-in-Aid for the JSPS Fellows (13J01596) and JSPS KAKENHI (24244058).

[1] M. Fiebig, J. Phys. D **38**, R123 (2005).
[2] S.-W. Cheong and M. V. Mostovoy, Nat. Mater. **6**, 13 (2007).
[3] T. Kimura, Annu. Rev. Mater. Res. **37**, 387 (2007).
[4] Y. Tokura, S. Seki, and N. Nagaosa,Rep. Prog. Phys. **77**, 076501 (2014).
[5] Y. Kitagawa, Y. Hiraoka, T. Honda, T. Ishikura, H. Nakamura, and T. Kimura, Nat. Mater. **9**, 797 (2010).
[6] W. J. Merz, Phys. Rev. **76**, 1221 (1949).
[7] N. Lee, C. Vecchini, Y. J. Choi, L. C. Chapon, A. Bombardi, P. G. Radaelli, and S. W. Cheong, Phys. Rev. Lett. **110**, 137203 (2013).
[8] R. D. Johnson, L. C. Chapon, D. D. Khalyavin, P. Manuel, P. G. Radaelli, and C. Martin, Phys. Rev. Lett. **108**, 067201 (2012).
[9] T. Aoyama, K. Yamauchi, A. Iyama, S. Picozzi, K. Shimizu, and T. Kimura, Nat. Commun. **5**, 4927 (2014).
[10] T. Kimura, T. Goto, H. Shintani, K. Ishizaka, T. Arima, and Y. Tokura, Nature (London) **426**, 55 (2003).
[11] H. Katsura, N. Nagaosa, and A. V. Balatsky, Phys. Rev. Lett. **95**, 057205 (2005).
[12] M. Kenzelmann, A. B. Harris, S. Jonas, C. Broholm, J. Schefer, S. B. Kim, C. L. Zhang, S.-W. Cheong, O. P. Vajk, and J. W. Lynn, Phys. Rev. Lett. **95**, 087206 (2005).
[13] I. A. Sergienko and E. Dagotto, Phys. Rev. B **73**, 094434 (2006).
[14] S. Picozzi, K. Yamauchi, B. Sanyal, I. A. Sergienko, and E. Dagotto, Phys. Rev. Lett. **99**, 227201 (2007).
[15] K. Noda, S. Nakamura, J. Nagayama, and H. Kuwahara, J. Appl. Phys. **97**, 10C103 (2005).
[16] C. R. dela Cruz, B. Lorenz, Y. Y. Sun, Y. Wang, S. Park, S.-W. Cheong, M. M. Gospodinov, and C. W. Chu, Phys. Rev. B **76**, 174106 (2007).
[17] J. Baier, D. Meier, K. Berggold, J. Hemberger, A. Balbashov, J. A. Mydosh, and T. Lorenz, J. Magn. Magn. Mater. **310**, 1165 (2007).
[18] X. Rocquefelte, K. Schwarz, P. Blaha, S. Kumar, and van den Brink, Nat. Commun. **4**, 2511 (2013).
[19] T. Kimura, S. Ishihara, H. Shintani, T. Arima, K. T. Takahashi, K. Ishizaka, and Y. Tokura, Phys. Rev. B **68**, 060403(R) (2003).
[20] T. Goto, T. Kimura, G. Lawes, A. P. Ramirez, and Y. Tokura, Phys. Rev. Lett. **92**, 257201 (2004).
[21] N. Tateiwa and Y. Haga, Rev. Sci. Instrum. **80**, 123901 (2009).
[22] H. K. Mao, P. M. Bell, J. W. Shaner, and D. J. Steinberg, J. Appl. Phys. **49**, 3276 (1978).
[23] T. Aoyama, A. Miyake, K. Shimizu, and T. Kimura, J. Phys. Soc. Jpn. **81**, SB036 (2012).
[24] T. Arima, T. Goto, Y. Yamasaki, S. Miyasaka, K. Ishii, M. Tsubota, T. Inami, Y. Murakami, and Y. Tokura, Phys. Rev. B **72**, 100102(R) (2005).

[25] Y. Yamasaki, H. Sagayama, N. Abe, T. Arima, K. Sasai, M. Matsuura, K. Hirota, D. Okuyama, Y. Noda, and Y. Tokura, Phys. Rev. Lett. **101**, 097204 (2008).

[26] T. Kimura, G. Lawes, T. Goto, Y. Tokura, and A. P. Ramirez, Phys. Rev. B **71**, 224425 (2005).

[27] H. Kuwahara, K. Noda, J. Nagayama, and S. Nakamura, Physica B **359**, 1279 (2005).

[28] T. Goto, Y. Yamasaki, H. Watanabe, T. Kimura, and Y. Tokura, Phys. Rev. B **72**, 220403(R) (2005).

[29] F. Kagawa, M. Mochizuki, Y. Onose, H. Murakawa, Y. Kaneko, N. Furukawa, and Y. Tokura, Phys. Rev. Lett. **102**, 057604 (2009).

[30] O. L. Makarova, I. Mirebeau, S. E. Kichanov, J. Rodríguez-Carvajal, and A. Forget, Phys. Rev. B **84**, 020408 (2011).

[31] A. Muñoz, M. T. Casáis, J. A. Alonso, M. J. Martínez-Lope, J. L. Martínez, and M. T. Fernández-Díaz, Inorg. Chem. **40**, 1020 (2001).

[32] K. Yamauchi, F. Freimuth, S. Blügel, and S. Picozzi, Phys. Rev. B **78**, 014403 (2008).